EFFICIENCY AND RESOLUTION OF GERMANIUM DETECTORS AS A FUNCTION OF ENERGY AND INCIDENT GEOMETRY

R.M. Keyser

New Product Development, ORTEC, 801 South Illinois Avenue, Oak Ridge, TN 37831

1 INTRODUCTION

The use of germanium detectors for the identification and quantification of radionuclides in unknown and non-standard counting geometries has increased in the recent past with the need to clean up and verify sites used for radionuclide processing, smuggling detection and other purposes. The calculation of the amount of radionuclide present requires a knowledge of the efficiency of the detector in the counting geometry. Several methods of determining the efficiency in these unusual geometries have been developed over the years. These methods are used in waste measurement, field (in situ) measurements and material verification. One method currently being used is the modeling of the detector response using Monte Carlo simulation programs, especially Monte Carlo N-Particle Code (MCNP). The input to MCNP is a detailed knowledge of the detector construction details, detector crystal details and the source being measured. This paper addresses the difficulty in obtaining the required detector crystal details, even when the common specifications are well known.

In addition, the Institute of Electrical and Electronic Engineers (IEEE) Germanium Test Standard (325-1996) is widely used for the specification of High Purity Germanium (HPGe) detectors. The two important specifications are the efficiency and the resolution of the detector. However, the IEEE 325-1996 standard only specifies the Full Width at Half Maximum (FWHM) measurement at one geometry and two energies. Thus, this standard does not apply in most counting geometries used today, especially for environmental samples.

Modeling programs, such as MCNP, use the physical dimensions of the detector crystal to predict the response of HPGe detectors on the assumption that the detector response can be related to the physical dimensions and that the detector crystal response is independent of the position of the interaction in the crystal. Other investigators[1], have shown that the peak resolution (FWHM, FW.1M and FW.02M) change with position of the incident gamma ray on the front of the detector. Such variability has possible implications for the accuracy of peak shape and area determination, since the calibration is potentially a function of angle of incidence.

To demonstrate that the efficiency and resolution vary as a function of energy and gamma-ray point of incidence, measurements have been made on several coaxial detectors of various crystal types and sizes for different energies. The full-energy peaks from 60 keV to 2.6 MeV were used.

2 EXPERIMENTAL SETUP

Several detectors were chosen as being representative of the majority of detectors in use today. Large detectors were selected as it was expected that these would show the most variation. However, it is shown that the variations are most significant in older detectors. The detectors were placed in a low-background shield to reduce any contribution from external sources. None of the detectors tested was a low-background type. The detector dimensions are shown in Table 1.

The sources used were ^{241}Am and ^{60}Co point sources. The ^{241}Am source was collimated to a 1 mm diameter beam by a 3 cm long by 17 mm diameter lead collimator. The ^{60}Co source was collimated to a 2 mm diameter beam by a 8 cm long by 8 cm diameter tungsten collimator. In addition, ^{60}Co data were

Table 1. Detectors Studied		
Detector Number	Diameter (mm)	Length (mm)
N21240A	60.5	60.4
N31626B	53.0	47.8
P41075A	84.5	100.5
P41182A	86.1	112.4
P41181A	81.5	53.7

collected without a collimator. Complete details of the collimators were presented earlier[2].

The measurements were made on the top or front of the detector in East-West and North-South modes and on the side of the detector in Up-Down mode as shown in Fig. 1. The actual positions were selected at random with respect to the crystal orientation.

The spectra were collected with a Digital Signal Processing MCA (DSPEC Plus), with 12 μs rise time (corresponding to an analog shaping time of about 6 μs), 1 μs flattop and a cusp of 1. The deadtime was always less than 10%. The number of channels was 16k, giving at least 6 channels in the FWHM of the narrowest 59 keV peak.

The peak areas and widths were calculated using the methods described in IEEE 325-1996 (equivalent to International Electrotechnical Commission standard IEC 61976-2000). The position numbers are arbitrary scale readings and are related to the detector crystal position by the count rate data.
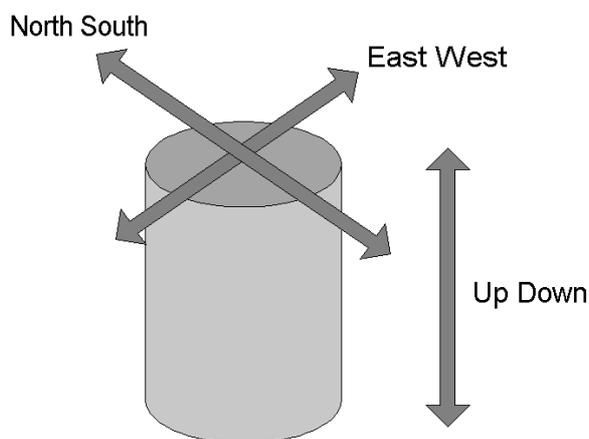
Figure 1. *Definition of Scan Directions*

3 RESULTS

3.1 Efficiency at 59 keV

The first detector studied was an ORTEC GMX type (n-type) with dimensions of 60 mm diameter and 60 mm length. The [241]Am scan on the front is shown in Fig. 2. The crystal diameter is shown by the black bar. Note the uniform sensitivity across the front of the detector, indicating that the crystal has uniform dead layer on the front.

Figure 2. *Peak Area vs Position on Front for 59 keV in NS Direction*

The scan down the side of a similar detector is shown in Fig. 3. This shows the 59 keV peak area for the Up-Down scans for 0 degrees and 90 degrees. The intensity of the peak shows the three thick regions in the mounting cup of the detector. More importantly, the two scans are nearly the same. The slight variation between the front of the crystal (left side) and the bottom of the crystal in the reduction in count with position is attributed to the increase in material at the bottom of the mounting cup. The peak area in the regions where the cup is thin, show that the dead layer is uniform along the length of the crystal. Other GMX detectors showed the similar results.

Figure 3. *Peak Count Rate at 59 keV vs Position on Side of Detector*

The relative dead layer was also measured for larger ORTEC GEM type detectors. Fig. 4 shows the relative intensity of the 59 keV peak for a scan along the length (UD) of the crystal. For comparison, the results of Ref. 3 for a similar, but not identical, detector are shown. Note that the first thick band is visible, but the second band is obscured by the thickening dead layer. In both of these detectors, the dead layer appears to be constant for a portion of the detector (starting at the closed end or front) and then increasing in thickness from some point
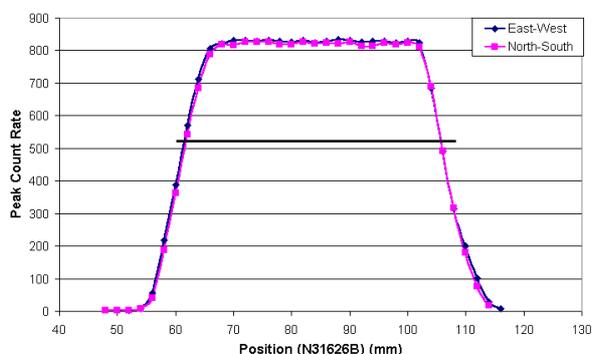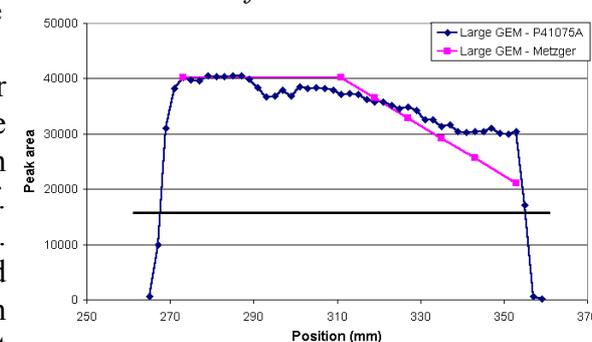

Figure 4. *Peak Count Rate at 59 keV vs Position on Side of Detector P41075A*

to the bottom of the crystal.

In contrast to these two detectors, Fig. 5 shows a 59 keV scan of another GEM detector, again of similar length and diameter. In this scan, both the thick bands of the cup can be seen and the dead layer is otherwise nearly uniform from front to rear of the crystal.

3.2 Resolution at 59 keV

The peak shape of ^{241}Am on the front of a GMX (N31626B) is shown in Fig. 6. The crystal diameter is shown by the black bar. Another detector is shown in Fig. 7. Note the uniformity of the peak shape over the front, with the exception of the increase for a region in Fig. 7 and the general broadening near the edges of the crystal.
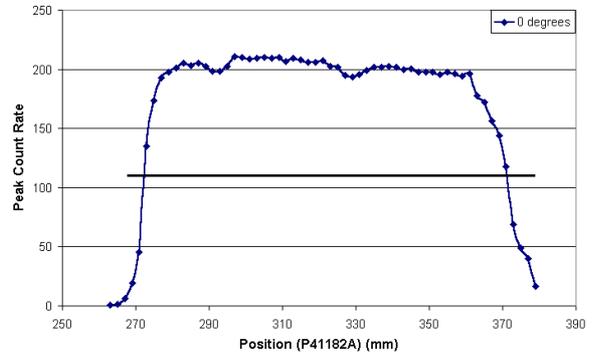
Figure 5. *Peak Count Rate at 59 keV vs Position on Side of Detector for P41182A*
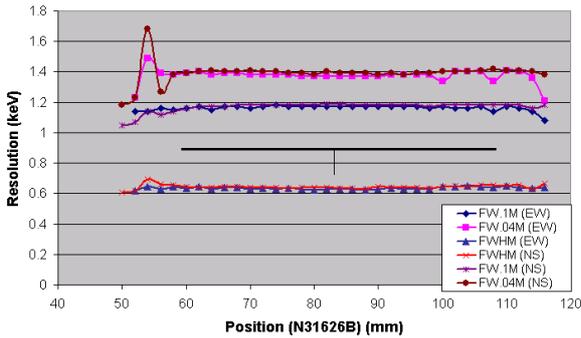
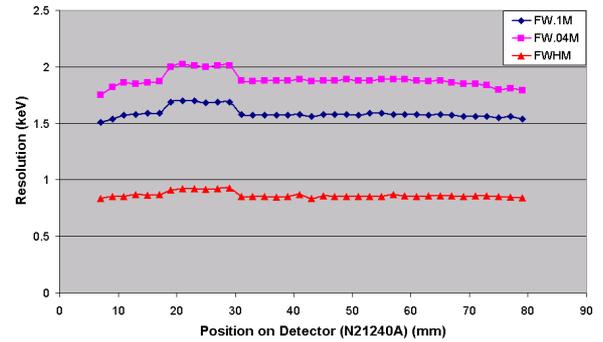**Figure 6**. *Resolution at 59 keV Across Front of GMX (N31626B).*

Figure 7. *Resolution at 59 keV Across Front of GMX (N21240A).*

The peak FWHM for the scans down the length of the crystal are shown Figs. 8, 9, and 10. These are again uniform, except for small variations at the ends of the crystals and at some positions down the length. With the exception of Fig. 7, it is expected that the detectors would exhibit this behavior because the low-energy gamma rays interact near the surface.
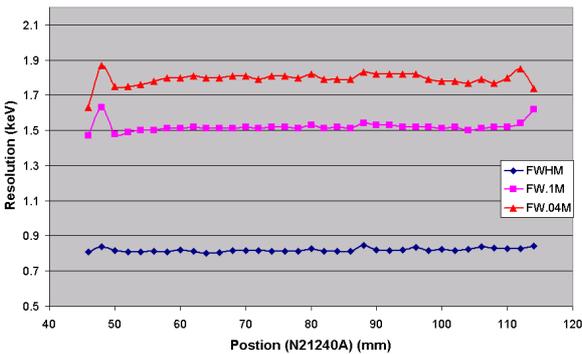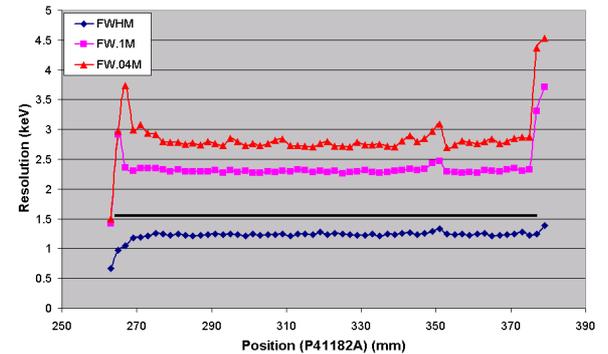
Figure 8. *Resolution at 59 keV the Side of GMX (N20140A).*

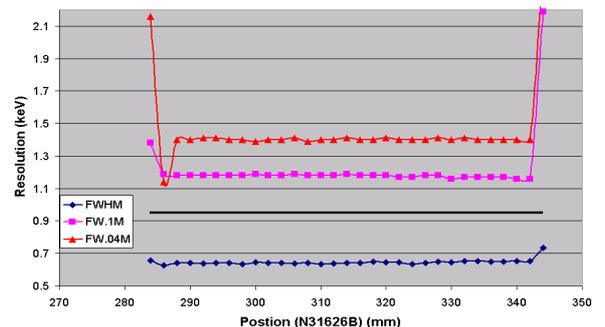**Figure 9**. *Resolution at 59 keV on the Side of GEM (P41182A).*

Figure 10. *Resolution at 59 keV on the Side of GMX (N31626B).*

3.3 Resolution at 1.1 and 1.3 MeV

The resolution for the ^{60}Co peaks for scans across the front of a GMX detector is shown in Fig. 12. The GMX detectors do not show the increase in width at the center of the crystal, as seen by previous workers. The broadening of the peak near the center of the crystal is due to the center hole of the detector. This hole extends to about 9 mm of the front surface, giving the possibility of loss of energy into the hole.
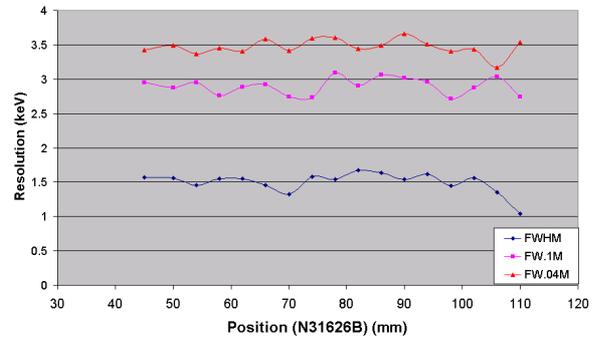
Figure 11 *Resolution at 1332 keV Across Front of GMX (N31626B).*

The ^{60}Co scans across the front for the GEM detectors are shown in Figs. 12 and 13.   Note that these scans show the same dependance of the FW.1M and FW.04M with front position as seen before. The 1173 and 1332 keV peaks show similar results. This is a general increase in peak width, but is more pronounced at the base of the peak.
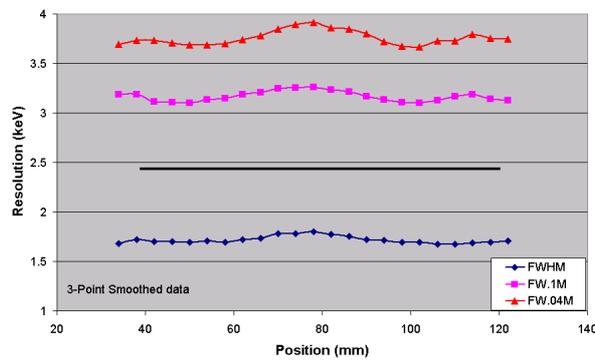
Figure 12 *Resolution at 1332 keV Across Front of GEM (P41075A).*
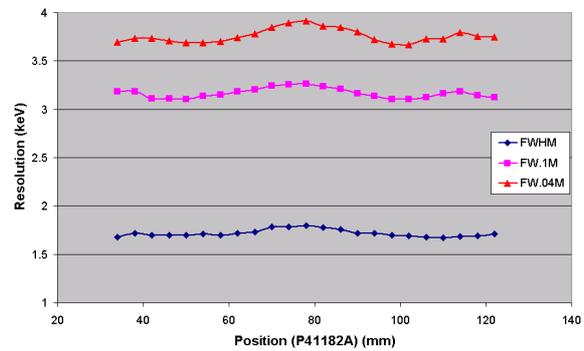
Figure 13 *Resolution at 1332 keV Across Front of GEM (P41182A).*

The scan on the side for GEM detectors is shown in Figs. 14 and 15. The shape is very nearly constant over the length except at the bottom of the crystal for Fig. 14, but begins to significantly increase about 75% of the distance from the top in Fig. 15.
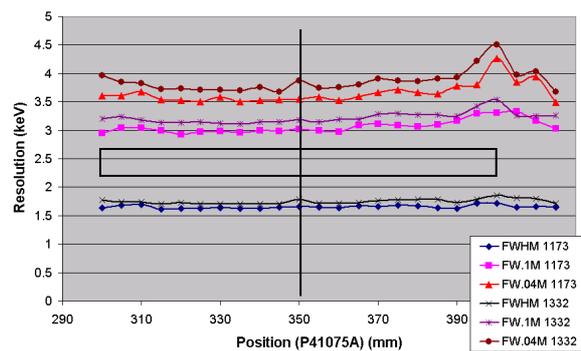
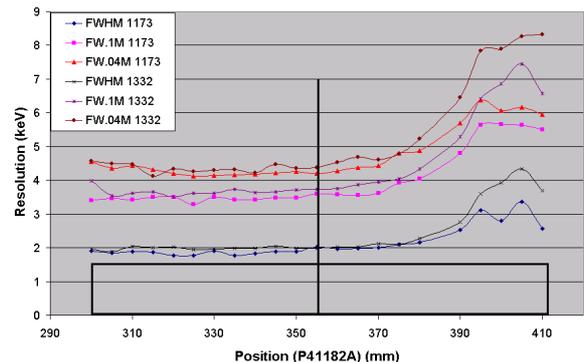**Figure 14**. *Resolution at 1332 on Side of GEM (P41075A).*

Figure 15. *Resolution at 1332 on Side of GEM (P41182A).*

3.4 Efficiency at 1.1 and 1.3 MeV

The sensitivity scan UD of a GEM detector for both 1173 and 1332 keV is shown in Fig. 16. This is the same detector and position as the detector in Fig. 14. The 1173 and 1332 keV UD scan has been plotted UD and DU to show the similarity between the front and rear of the crystal. This plot shows the sensitivity is uniform away from the ends of the crystal.

Fig. 17 shows the same plot for the GEM detector in Fig. 15. The 1173 and 1332 keV UD scan has been plotted UD and DU. Note that the detector is very symmetric top-to-bottom, which is not seen in the 59 keV scan (Fig. 4).
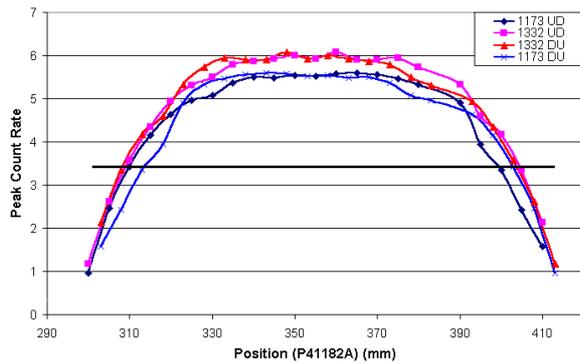

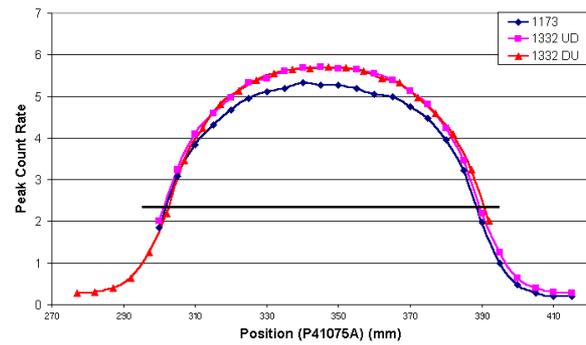**Figure 16**. *Peak Count Rate at 1173 and 1332 keV vs Position on Side of Detector P41182A*

Figure 17. *Peak Count Rate at 1173 and 1332 keV vs Position on Side of Detector P41075A*

4 DISCUSSION and CONCLUSION

Previous workers[1,3] measured several detectors in preparation for use in MCNP and other programs. These scans showed significant variation in the sensitivity (efficiency) and peak shape with the incident position of the gamma-ray beam. Detectors from several manufacturers were used. In one work, the actual thickness of the dead layer as a function of the position on the detector crystal surface was very important to the measurement geometry.

These variations could have a significant impact on the efficacy of the calculations. Thus it is important to measure the variation for more detectors.

The peak shape and sensitivity for the detectors studied did not show the wide variations with incident beam position as seen by others. However, similar detectors, in terms of easily measured physical properties (length and diameter), do show this variation. Thus, any model of a detector performance will, of necessity, require a very precise characterization of the exact detector. Future work on other detectors will extend these measurements and compare the MCNP predictions for different assumptions with experimental results.

REFERENCES

1. R. J. Gehrke, R. P. Keegan, and P. J. Taylor, "Specifications for Today's Coaxial HPGe Detectors," 2001 ANS Annual Meeting, Milwaukee, WI

2. R. M. Keyser, "Resolution and Sensitivity as a Function of Energy and Incident Geometry for Germanium Detectors", 2002 IRRMA Meeting, June 2002, Bologna, Italy

3. R. L. Metzger, private communication, see also: R. L. Metzger, K. A. Van Riper, and K. J. Kearfott, "Radionuclide Depth Distribution by Collimated Spectroscopy," 2002 ANS Topical Meeting, Santa Fe, NM